Cellulose (2023) 30:4941–4955
https://doi.org/10.1007/s10570-023-05200-0

ORIGINAL RESEARCH

Elucidating the characteristics of a promising nitrate ester polysaccharide derived from shrimp shells and its blends with cellulose nitrate

Ahmed Fouzi Tarchoun · Djalal Trache · Mohamed Abderrahim Hamouche · Amir Abdelaziz · Hani Boukeciat · Imene Chentir · Sabri Touidjine · Thomas M. Klapötke

Received: 12 January 2023 / Accepted: 10 April 2023 / Published online: 18 April 2023

Abstract Recently, polysaccharides have attracted tremendous interest as potential candidates to develop promising high-energy dense polymers through the chemical functionalization of their structures. Therefore, chitosan nitrate (CSN), as an energetic polysaccharide was fabricated by nitration of chitosan (CS) derived from shrimp *Parapenaeus longirostris* shells. The physicochemical, structural, and thermal features of the designed energetic CSN and its precursors were elucidated by density measurements, elemental analysis, FTIR, SEM, TGA, and DSC experiments. The mechanical sensitivities and calorific energy of the produced CSN were also determined and its theoretical detonation performance was computed using the EXPLO5 V6.04 software. The results demonstrated the efficiency of the performed method to produce the desired CSN with attractive characteristics such as a density of 1.701 g/cm^3, nitration content of 16.55%, impact sensitivity of 15 J, heat of combustion of 10,610 J/g, detonation velocity of 7764 m/s, and specific impulse of 242 s, which are better than those of commonly used nitrocellulose (NC). Besides that, new energetic CSN/NC polymer blends with different mass ratios (CSN:NC (wt%) = 25:75, 50:50, and 75:25) were elaborated and characterized in terms of their chemical structure, thermal behavior, and energetic performance. Experimental findings highlighted the attractive properties of the developed CSN/NC blends, providing evidence for the excellent synergistic effect between energetic CSN and NC polymers. Finally, this work established that shrimp shells wastes could serve as valuable biomass for the production of promising insensitive and high-energy dense polysaccharide, which is expected to be widely employed in the next generation of energetic formulations.

Keywords Shrimp shells, extraction, chitosan · Nitration · Nitrocellulose · Energetic blend

A. F. Tarchoun (✉)
Energetic Propulsion Laboratory, Teaching and Research unit of Energetic Processes, Ecole Militaire Polytechnique, BP 17, Bordj El-Bahri, 16046 Algiers, Algeria
e-mail: tarchounfouzi@gmail.com

A. F. Tarchoun · D. Trache (✉) · M. A. Hamouche · A. Abdelaziz · H. Boukeciat · S. Touidjine
Energetic Materials Laboratory (EMLab), Teaching and Research unit of Energetic Processes, Ecole Militaire Polytechnique, BP 17, Bordj El-Bahri, 16046 Algiers, Algeria
e-mail: djalaltrache@gmail.com

I. Chentir
Food Laboratory, Processing, Control and Agriresources Valorisation, Ecole Supérieure des Sciences de l'Aliment et des Industries Agroalimentaires, 16200 Oued Smar, Algiers, Algeria

T. M. Klapötke
Department of Chemistry, Ludwig Maximilian University, Butenandtstrasse 5–13 (D), D-81377 Munich, Germany

Introduction

Recently, the world has been affected by a considerable increase in petroleum costs combined with predictions of future scarcity and unavailability. In this regard, the valorization of sustainable and renewable biomass for the development of energy-rich materials has become a vast area of research globally (Reshmy et al. 2022; Tarchoun et al. 2022c). Among the accessible renewable and sustainable biomaterials, a special focus has been given to the exploration of polysaccharides as promising alternative biopolymers to substitute non-biodegradable and toxic fossil fuels (Nasrollahzadeh et al. 2021; Mohanty et al. 2022). Plentiful sustainable and environmental-friendly polysaccharides comprising cellulose, chitin/chitosan, starch, gum, alginate, and pectin have garnered substantial interest for applications in several industrial sectors owing to their outstanding structural and physicochemical features, biocompatibility, abundant availability, ease of modification, and promising potentials (Nasrollahzadeh et al. 2021). Among the interesting naturally occurring polysaccharides, chitosan (CS) is the second most abundant carbohydrate biopolymer on earth after cellulose, and it is conventionally prepared by deacetylation of chitin (CT) under alkaline treatments (Negm et al. 2020; Rashki et al. 2021). Structurally, CS is a linear polyaminosaccharide of β-(1,4)-linked *D*-glucosamine units, with the main difference compared to the chemical structure of cellulose and chitin is the presence of primary amine (NH_2) functional group, bonded to the C2 positions, rather than hydroxyl and acetyl groups, respectively. Importantly, this reactive amino functionality-bearing CS has become an ideal support, compared to other biopolymers, for its unique applications to design innovative bio-based products with advanced functionalities (Flórez et al. 2022; Bhardwaj et al. 2021). Regarding the production area, the CS market is escalating exponentially, expected to reach US$63 billion by 2024, while crustaceans (e.g. lobsters, shrimp, crabs, krill, barnacles, crayfish) are the most widely exploited sources to meet the growing demand (Joseph et al. 2021; Begum et al. 2021). In fact, the Algerian coastline, which extends over 1200 km of the Mediterranean, constitutes an ecological system rich in shrimps of *Parapenaeus longirostris* variety, which is a potential underutilized source of CT and CS (Benhabiles et al. 2012; Ben Seghir and Benhamza 2017). Therefore, the valorization of the discarded remnants from shrimp shells can become, in case of investment, a center of crucial economic interest for the industry of CT- and CS-based derivatives. Depending on the biomass source, different purification and pretreatment processes are performed to generate CT, which will be subsequently used to produce CS (Mohan et al. 2020; Huet et al. 2021). Conventionally, the preparation procedure of CS usually requires three main stages, which are (I) demineralization, (II) deproteinization and deacetylation reactions, respectively (El Knidri et al. 2018). The first step focuses on the elimination of minerals such as magnesium and calcium carbonates using mineral acid, whereas the second one consists of removing proteins through alkaline treatment. In certain extraction procedures, bleaching treatment with organic solvent is also performed to remove pigments (Pal et al. 2021). The deacetylation of CT to produce CS is usually achieved by alkaline hydrolysis of the acetamide groups. Based on the degree of deacetylation (DDA), CS can be classified into a low-deacetylated CS (DDA: 50–70%) and high- deacetylated CS (DDA: 70–99%), opening an extensive range of possibilities to produce CS with tailored features, which have broadened its usage as a promising nitrogen-rich polysaccharide in a wide spectrum of fields such as food, medicine, pharmaceutics, electronics, biofuels, and will undoubtedly continue to find ways to other emerging uses (Joseph et al. 2021; Ahmad et al. 2020).

Regarding the research area of energetic polysaccharides, nitrate ester cellulose, commonly known as nitrocellulose (NC), has been so far the most popular energy-rich polymer used in multiple civilian and defense sectors owing to its attractive performance such as high energy, explosiveness, and good compatibility with other additives (Dou et al. 2022; Trache and Tarchoun 2019). In addition to NC, several new cellulose-based energetic polymers with enhanced performance have been synthesized and studied (Dou et al. 2022). For instance, it is demonstrated in our recent investigations that the structural and molecular modifications of the basic structure of ordinary cellulose are a powerful methodology to develop new energetic cellulose-rich polymers such as nitrated amine-functionalized cellulose, nitrated carbamate-modified cellulose, and nitrated azide-functionalized cellulose, which possess potential applications in the

fields of solid propellants and explosives (Tarchoun et al. 2020a, 2021b, 2022d). Therefore, the highly attractive performance obtained for the developed energetic cellulosic materials has motivated us to investigate other reactive polysaccharides, mainly CS, to pave the way toward the next generation of high-energy polymers.

To the best of our knowledge, a few attempts have been undertaken to convert CS into energetic chitosan nitrate (CSN) derivatives. Hirano in 1986, synthesized nitrochitosan by nitration of natural CS using fuming nitric. Two decades later, Liu et al. (2001) and Zhang et al. (2003) prepared CSN with an acid procedure in order to be employed as an intermediate for semi-interpenetrating polymer network production. Actually, CSN is utilized in the removal process of heavy metals, as a cross-linking agent, and in electrochemical devices (Rahman et al. 2019; Jha et al. 2013). However, the adopted nitration method in the previously mentioned references produced CSN with a low nitration level, which strongly affects its properties and applicability features as a high-energy polysaccharide. As a consequence, highly nitrated chitosan has been recently designed through electrophilic nitration of commercially available CS (Li et al. 2020; Tarchoun et al. 2022b). Compared to the conventional NC, this energetic nitrogen-rich polysaccharide demonstrated improved energetic performance with great potential application in solid rocket propellants and composite explosives. The outstanding characteristics of highly substituted CSN have also encouraged us to investigate its blending with NC and scrutinize the characteristics of the obtained energetic CSN/NC composites, which is expected to be an excellent reference for the development of new high-performance formulations based on nitrated polysaccharides.

The novelty of the current work is the valorization of marine co-products, particularly the *Parapenaeus longirostris* shrimp shells generated after food processing, to develop a promising insensitive and high-energy dense polysaccharide through electrophilic nitration of the extracted chitosan. The produced energetic CSN and its corresponding precursors were subjected to several structural and thermal analyses. Moreover, the sensitivity features, the heat of combustion, and the detonation performance of the designed CSN have been determined and compared to those of conventional nitrocellulose. In addition, new energetic polymer blends based on CSN and NC were fabricated and deeply characterized to offer helpful guidelines for their potential utilization in composite explosives and solid propellants.

Experimental section

Materials

In this study, the discarded remnants from shrimp *Parapenaeus longirostris* shells after food processing were employed as raw material to extract CT and CS derivatives. NC, with a nitrogen content of 12.61%, was synthesized at EMLab as previously mentioned by Tarchoun et al. (2021b). Hydrochloric acid (HCl, 37%), sodium hydroxide (NaOH), hydrogen peroxide (H_2O_2, 30%), fuming nitric acid (HNO_3), acetic anhydride (Ac_2O), and sodium bicarbonate ($NaHCO_3$) were purchased from VWR-Prolabo and used without further purification.

Preparation procedure of chitosan nitrate

The shrimp waste was collected and the shells were thoroughly washed with distilled water to remove all impurities, followed by prolonged air-drying for two weeks. The dried shrimp shells were ground to a fine powder. Next, chitin (CT) was extracted following a multistep process. Firstly, demineralization was performed using 1 M HCl at a solid-to-liquor ratio of 1/30 (w/v), followed by deproteinization with 3 M NaOH at the same ratio (Srinivasan et al. 2018). CT, without pigments, was obtained after treatment with 15% H_2O_2 at a solid: liquid ratio of 1:100 (w/v). Each extraction step was carried out under agitation at room temperature for 75 min and followed by washing with distilled water, filtration, drying and finally grinding. After that, the isolated CT, with a yield of 25.63% and density of 1.551 ± 0.003 g/cm^3, was deacetylated, through alkali hydrolysis, using 50% NaOH at 80 °C for 4 h under stirring (Srinivasan et al. 2018; Marei et al. 2016; Teli and Sheikh 2012). The deacetylation was repeated two times, and the obtained solid residue was then successively washed with distilled water and ethanol until neutral PH, and oven-dried in an oven to afford the corresponding CS (yield of 88.79% and density of 1.564 ± 0.002 g/cm^3) with DDA of 88.43 ± 0.84%. CT: Anal. found (%): C

46.58, H 6.25, N 6.64; calcd. (%): C 47.29, H 6.40, N 6.90. CS: Anal. found (%): C 43.84, H 6.25, N 8.21; calcd. (%): C 44.72, H 6.83, N 8.70.

Lastly, chitosan nitrate was synthesized according to the method described in our recent paper (Tarchoun et al. 2022b). Briefly, the nitration reaction was carried out in an ice bath for 5 h in an aqueous Ac_2O solution using fuming HNO_3 as a nitrating agent. The proportions used were 1/7 (w/v) CS to HNO_3 and 1/1 (v/v) Ac_2O to HNO_3. The mixture was then filtered and the resulting product was neutralized, respectively, by a solution of $NaHCO_3$ (2%, w/v) and distilled water in order to remove residual acids. The neutralization process was accomplished at 80 °C for 2 h, and the final product was filtered and dried under vacuum. The experimental procedure of the preparation is illustrated in Fig. 1. CSN: Anal. found (%): C 23.83, H 2.48, N 16.55; calcd. (%): C 24.32, H 2.70, N 18.92.

Elaboration of CSN/NC blends

With the aim of studying the synergistic effect of CSN and NC, energetic CSN/NC polymer blends with different mass ratios (CSN: NC (wt%) = 25:75, 50:50, and 25:75) were elaborated. As depicted in Fig. 1, well-determined amounts of the dried samples were dissolved in acetone under stirring at room temperature. The solution was then poured into a petri dish and dried in the open air until solvent evaporation, and the considered composites were recovered. The samples are labeled as CSN 25% NC 75%, CSN 50% NC 75%, and CSN 75% NC 25%.

Apparatus and methods

Fourier transform infrared spectroscopy (FTIR) was carried out with a Perkin Elmer 1600 spectrometer within the wavenumber range of 4000 − 400 cm^{-1} by averaging 32 scans at a resolution of 4 cm^{-1}. Elemental analyses were recorded using a Vario III Elemental analyzer. Scanning electron microscopy (SEM) images were performed with scanning electron microscopy (SEM) of Carl Zeiss SIGMA. Experimental densities were measured using an electronic Accypyc 1340 II densimeter. Thermogravimetric Analysis (TGA) and differential scanning calorimetry (DSC) experiments for about 1–2 mg samples under nitrogen gas were conducted using Perkin-Elmer TGA 8000 and DSC 8000 analyzers, respectively,

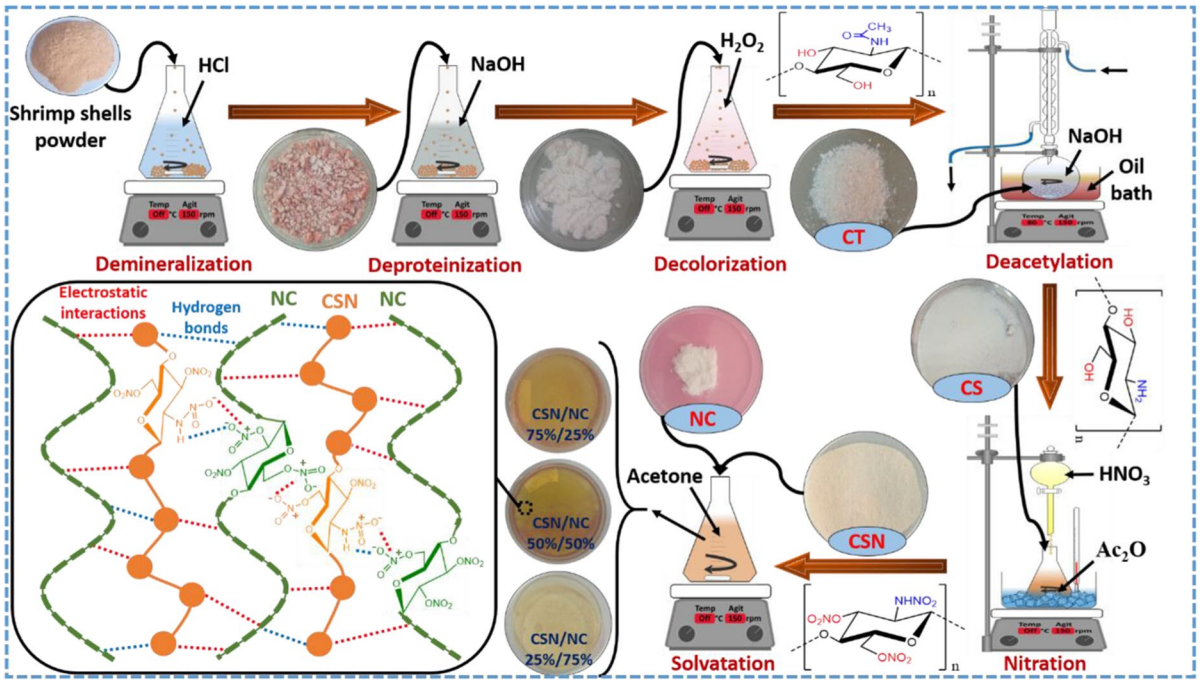

Fig. 1 Multistep preparation pathway of CSN from shrimp *Parapenaeus longirostris* shells and its energetic blends with NC

over the temperature range of 50–350°C at a heating rate of 10°C/min. Impact and friction sensitivities (IS and FS) were determined by BAM drop hammer and friction tester according to the STANAG 4489 and STANAG 4487, respectively (NATO 1999, 2002). The reported values of IS and FS correspond, respectively, to the lowest energy and force at which a positive result can be obtained from at least one out of six repeated tests. The heat of combustion ($\Delta_c U$) of the designed CSN and its blends with NC were measured using a Parr 6200 bomb calorimeter under 30 bar of oxygen atmosphere. Their theoretical energetic parameters were also predicted using the EXPLO5 (V6.04) thermodynamic code (Sućeska 2017).

Results and discussion

Physico-chemical properties of the extracted CT and CS

In this study, the CT yield, calculated by the dry weight ratio between the extracted chitin and raw shrimp shells, was found to be 25.63%, which is in good agreement with the values previously reported for CT isolated from crustaceans (Benhabiles et al. 2012; Saravana et al. 2018). Moreover, to further elucidate the characteristics of the isolated CT and CS, physicochemical analyses were performed to determine the density, nitrogen, moisture, and ash contents of each extracted sample (CT and CS). The measured experimental densities reveal that CS has a better density ($\rho = 1.564 \pm 0.002$ g/cm^3) than its CT precursor ($\rho = 1.551 \pm 0.003$ g/cm^3), indicating that the amine groups (NH_2) of CS contribute better to the density of this biopolymer than the acetyl function of CT. Furthermore, the nitrogen content of the prepared CT ($Nc = 6.64\%$) from local shrimp *Parapenaeus longirostris* shells is found to be close to the theoretical value ($Nc = 6.90\%$), calculated for completely acetylated CT, demonstrating its high purity and the effective removal of protein during deproteinization process (Saravana et al. 2018). It is also revealed that the nitrogen content increased from CT to CS ($Nc = 8.21\%$), which is attributed to the conversion of the acetamide ($–NHCOCH_3$) groups of CT to amino ($–NH_2$) ones during alkaline deacetylation (Benhabiles et al. 2012). Besides that, the moisture and ash contents of the investigated samples were determined according to the methods detailed in our previous paper (Tarchoun et al. 2019a). The moisture content of the extracted CT and CS are obtained as 3.35% and 5.89%, respectively, which falls within the acceptable United States Pharmacopoeia limit of moisture content ($\leq 7\%$) (Tarchoun et al. 2019a, b). These low values also indicate the suitability of the prepared CT and CS from local shrimp *Parapenaeus longirostris* shells as adsorbent derivatives for pharmaceutical and biomedical applications (Liakos et al. 2021). In addition, experimental results show that the obtained CT and CS contain reduced ash content (CT: 0.36% and CS: 0.68%) of less than 1%, indicating the reduced amount of calcium carbonates and other minerals from the original source, and confirming once more their high-quality grade (Trung et al. 2020; Phuong et al. 2022). Therefore, we can conclude that shells, derived from local shrimp *Parapenaeus longirostris* species, could be considered promising marine biomass to produce high-quality polysaccharides (CT and CS).

Structural characteristics

The chemical functionalities of the designed CSN and its CS and CT precursors were identified by infrared spectroscopy, and the obtained spectra are shown in Fig. 2a. The extracted CT exhibits the typical vibrational bands of N-acetylglucosamine units (2-acetamino-2-deoxy-β-d-glucopyranose), comprising O–H elongation at 3450 cm^{-1}, N–H stretching at 3280 cm^{-1} and 3097 cm^{-1}, C–H elongation at 2900 cm^{-1}, amide I stretching of C = O at 1655 cm^{-1} and –NH bending at 1628 cm^{-1}, amide II elongation of C–N band at 1550 cm^{-1}, asymmetric and symmetric CH_2 bending at 1378 − 1309 cm^{-1}, skeletal vibrations involving the C–O stretching at 1020–1080 cm^{-1}, and ß-1,4-glycosidic linkage vibration at 890 cm^{-1} (Kumari et al. 2017; Yuan et al. 2020). The CS spectrum is found to be similar to that of CT, with the most detailed difference related to the obvious decrease of the characteristic absorption bands of acetyl groups, consisting of the fact of a high DDA after alkali treatment. As a result, more NH_2 groups are exposed in the as-prepared CS sample. Furthermore, the spectra of the extracted CT and CS from local shrimp *Parapenaeus longirostris* shells are analogous to those of the commercially available chitin and chitosan (CT–C and CS–C) and those

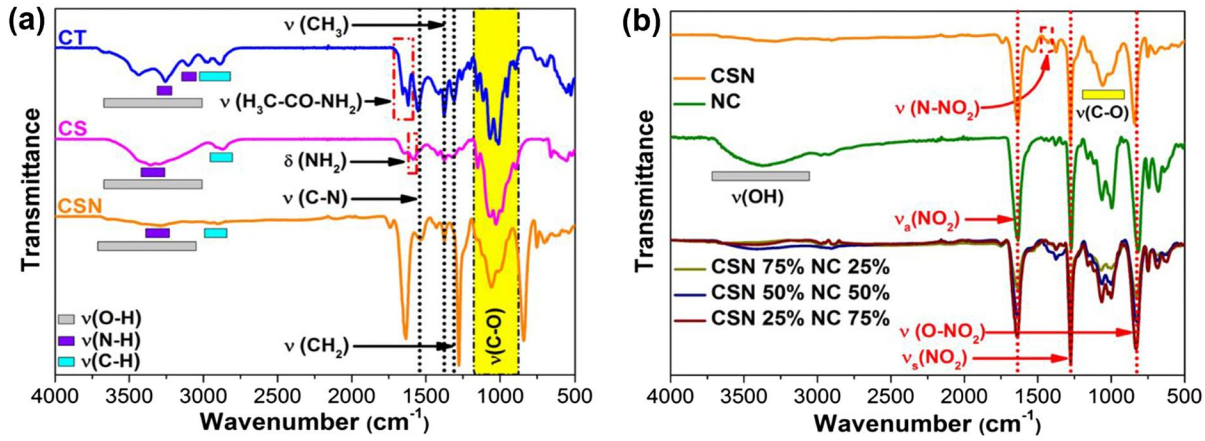

Fig. 2 FTIR spectra of **a** nitrated chitosan and its precursors; **b** energetic CSN/NC polymer blends

derived from other natural resources (Mohan et al. 2020; Aili et al. 2017; Doğdu et al. 2021). In addition, the degree of deacetylation of the prepared CS was calculated from the IR spectrum of CS by recording the absorbance at 1655 cm^{-1} for amide I (A_{1655}) and 3450 cm^{-1} for the OH group (A_{3450}), following the most appropriate method proposed by Domszy and Roberts (DDA (%) = [1- (A_{1655}/ A_{3450})/1,33] × 100) (Domszy and Roberts 1985; Kasaai 2008). It is important to point out that CS–C with a DDA of 98% is considered a reference to confirm the precision of this method. Compared to the value provided by the manufacturer, the calculated DDA of CS–C is found to be 97.43 ± 0.65%, justifying the excellent reliability of the followed IR approach. Interestingly, the prepared CS presents a high DDA of 88.43 ± 0.84%, indicating that the deacetylation efficiency of CT derived from shrimp shells is favorable compared to other raw biomass (Kumari et al. 2017; Francis et al. 2021). However, it must be taken into account that the DDA of the obtained CS depends on several factors, such as the nature of the organism from which it was extracted and the conditions employed in the extraction process. These supportive results demonstrate once more that the envisaged polysaccharides are successfully achieved with high purity.After nitration, we can reveal from Fig. 2a that the obtained CSN displays the typical IR profile of nitrocellulose, except for the occurrence of the weak N–NO_2 vibrational band at 1428 cm^{-1} in CSN (Tarchoun et al. 2022b; Li et al. 2020). Furthermore, it is clear that the significant changes that occurred in the molecular structure of CSN compared to its precursor corresponded to the appearance of the characteristic absorption peaks of nitro (NO_2) at 1640 cm^{-1} and 1280 cm^{-1}, and nitrate ester (O–NO_2) at 835 cm^{-1}, as well as the obvious decrease in the intensity of O–H and N–H bands. These results confirm the successful electrophile substitution of hydronium ions (H^+) of accessible hydroxyl and amine sites of glucosamine units with nitronium (NO_2^+) ones without the destruction of the main polymer framework during the whole nitration. Regarding the spectra of the developed CSN/NC blends plotted in Fig. 2b, most of the vibrational bands appeared at the same wavenumbers as presented in the CSN and NC, highlighting their excellent chemical compatibility. However, the disappearance of some vibrational bands of CSN in all CSN/NC spectra is attributed to their overlapping with NC peaks since the selected energetic polysaccharides have similar chemical structures. Other interesting results from Fig. 2b correspond to the intensification of the representative peaks of NO_2 and O–NO_2 as well as the decrease in the intensity of the OH band in CSN/NC blends as compared to raw CSN and NC, which can be explained by hydrogen bonding and electrostatic N–O interactions between the two energetic polymers. In this subject, some authors stipulated that these interactions would improve the safety performance of the prepared energetic mixture (Mezroua et al. 2022; Guo et al. 2017; Touidjine et al. 2022), as will be proved later through sensitivity measurements. Additionally, these outcomes highlight that no specific alteration in the chemical

structures of CSN or NC was caused by the fabrication process.

Morphological features

The morphology and surface physical state of the starting shrimp shells and their CT, CS, and CSN derivatives were analyzed using SEM to probe the eventual morphological changes caused by the performed chemical treatments. As can be seen from Fig. 3, the raw shrimp shell sample displays a tightly arranged structure, which may be due to the presence of attached chitin and protein layers and mineral salts (Zhao et al. 2019; Saravana et al. 2018). Indeed, according to previous studies, CT is a chief element of the shell reticular skeleton, and the inside flexible protein macromolecules are unevenly attached to the CT backbone, while inorganic compounds are toughly entrenched in CT chains (Lavall et al. 2007; Saravana et al. 2018). However, after chemical treatment, the isolated CT exhibits detached thin sheets with uniform lamellar structure, indicating that the performed extraction process leads to the removal of proteins and minerals from the shell of shrimp *Parapenaeus longirostris* wastes, and hence the CT sheets are obtained. An earlier report on the extraction of CT from crustacean waste showed that the parallel CT chains are arranged in bonded piles or sheets by hydrogen interactions through the amide groups (Saravana et al. 2018). After deacetylation, the obtained CS appears to have a rough irregular microstructure with rod-like aggregates, which is attributed to the alkaline hydrolysis during the deacetylation process that caused the disintegration of the crosslinking bonds between CT chains and the elimination of acetyl moieties (Phuong et al. 2022). It is interesting to point out that the microscale morphologies of the CT and CS, prepared in this work from shrimp *Parapenaeus longirostris* shells, are comparable to those obtained from deep-sea mud shrimp (Rasweefali

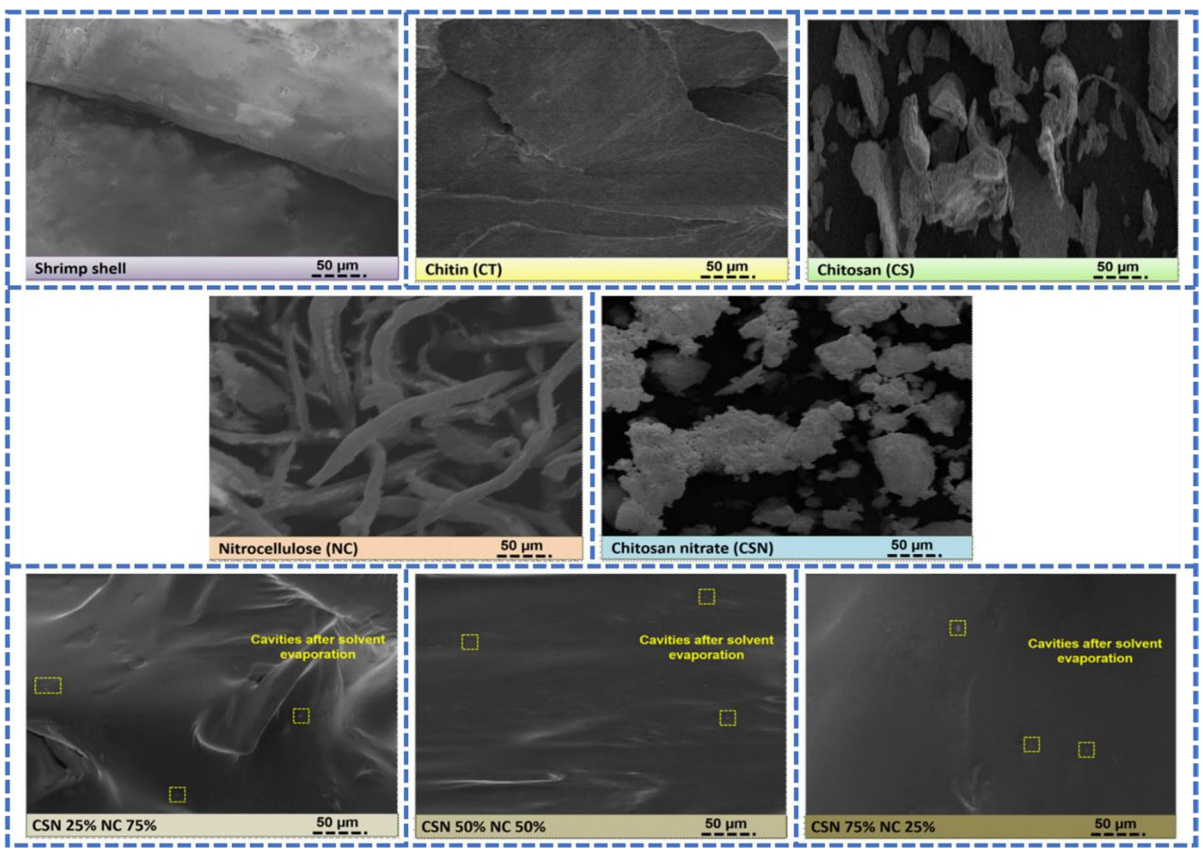

Fig. 3 SEM micrographs of the developed energetic CSN/NC polymer blends and their raw compounds

et al. 2021), Penaeus notialis shrimp shells (Olaosebikan et al. 2021), aquatic invertebrates (Kaya et al. 2014), and crab shells (Kumari et al. 2017). After nitration, CSN presents a rod-shaped and granular structure with a rougher surface and larger agglomeration, which is related to the chain bundling caused by the presence of electron-withdrawing O–NO_2 and N–NO_2 groups that cover the surface of glucosamine units. This finding also indicates that the performed nitration process leads to a uniform and homogenous distribution of NO_2 groups with a negligible morphological alteration.

In the case of the as-prepared energetic blends, it can be clearly noticed from Fig. 3 that all CSN/NC composites exhibit an eventual continuous phase system. Compared with that of CSN and NC, the microstructure of the prepared CSN/NC blends significantly changed from the irregular rod-shaped morphology of CSN and the fibrous aspect of NC to a uniform structure with a smooth surface. This finding highlights the effective dissolving process of CSN/NC mixtures to form dense matrices. Another interesting result is that the obtained sheet structure after the casting process is likely promoted by increasing the mass ratio of CSN. Such effective interfacial contact between the two energetic polymers is expected to improve the thermal decomposition performance of the energetic blends, as will be confirmed later in the paper by TGA and DSC analyses. Moreover, the observed small cavities at the sheet surface of CSN/NC blends are attributed to the evaporation of the tiny acetone drops already stacked at the surface. Besides that, all the prepared CSN/NC blends exhibit good continuity and no obvious defects are detected, demonstrating that they have good quality.

Thermal analysis by TGA

The thermal decomposition behavior of the investigated bio-based polymers (CT, CS, and CSN) derived from shrimp *Parapenaeus longirostris* shells biomass, as well as NC and the as-prepared CSN/NC blends were assessed by TGA, and the recorded thermograms are reported in Fig. 4. As can be perceived from TGA/DTG curves plotted in Fig. 4a, the extracted CT and CS present an initial small weight loss at 80–140 °C assigned to the moisture evaporation, followed by an important decomposition stage, in the temperature range of about 260–380 °C, attributed to the degradation of polysaccharide framework through multiple processes (Saravana et al. 2018; da Silva Lucas et al. 2021). In the first event, the amount of physically absorbed water of CS (5.3%) is found to be higher than that of CT (2.9%), which is probably due to the hygroscopic nature of amino groups when compared to the acetyl groups of CT (Luo et al. 2020). The second stage corresponds to the degradation of N-acetylated and deacetylated functional groups of CT and CS respectively, as well as the dehydration of their saccharide units. In accordance with the findings of Mohan et al. (Mohan et al. 2020), the onset and maximum peak temperatures of the extracted CS (T_{onset} = 265.6 °C and T_{peak} =

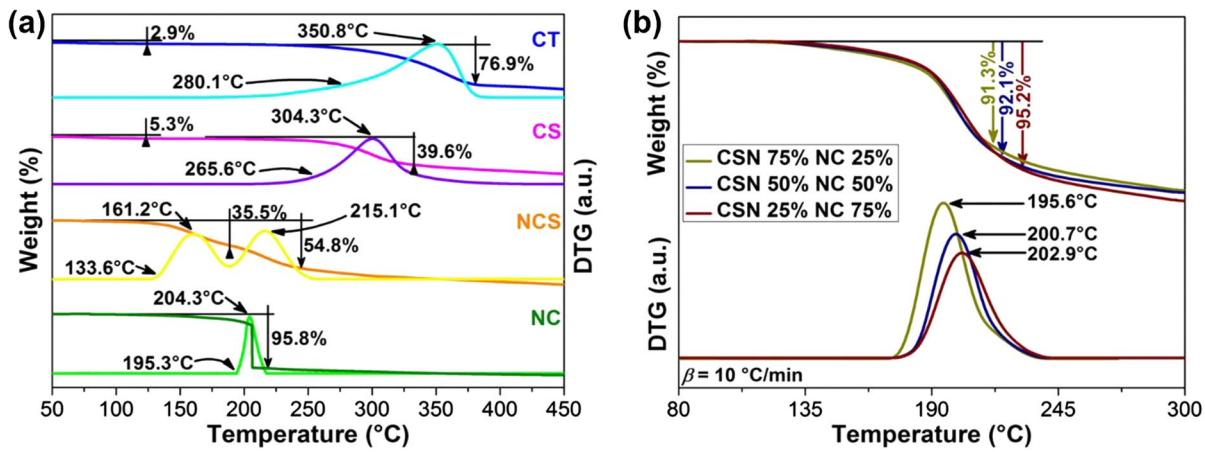

Fig. 4 TGA/DTG thermograms at $\beta = 10$ °C/min of **a** nitrated chitosan and its precursors; **b** CSN/NC blends

304.3 °C), shown in Fig. 4a, are lower than those of its corresponding CT (T_{onset} = 280.1 °C and T_{peak} = 350.8 °C). This finding is explained by the fact that the N-acetylated polymer units of CT are more thermally stable than the deacetylated units of CS. Moreover, the lower mass loss of the extracted CS (39.6%) compared to its CT precursor (76.9%) was expected as normally reported before, due to the cross-linking of CS during thermal decomposition (Muñoz-Nuñez et al. 2022; da Silva Lucas et al. 2021). In addition, it is interesting to point out that the thermal stability of CT and CS extracted in this work from shrimp shells (Parapenaeus longirostris) is found to be comparable to those from mealworm´s cuticles studied by da Silva Lucas. et al. (2021), those obtained from some insects reported by Mohan et al. (2020), and those prepared from the same shrimp species mentioned by Ben Seghir et al. (2017).

In the case of the synthesized CSN, two overlapping weight loss events were identified in the approximate temperature range of 115–240 °C, similar to the literature reports on the newly developed high-nitrated chitosan (Zhang et al. 2022; Tarchoun et al. 2022b). However, compared to the thermal stability of nitrochitosan reported in these previous papers, it appears from Fig. 4a that the CSN, prepared in this study from local shrimp *Parapenaeus longirostris* shells, shows enhanced thermal decomposition with 161.2 and 215.1 °C as maximum peak temperatures for the first and second decomposition events, respectively. Moreover, the first mass loss (35.5%), corresponded to the decomposition of explosophoric nitramines and nitrate esters, and the mass loss of the second event (54.8%), related to the decomposition of the polymeric skeleton, are found to be higher than those mentioned in our recent paper for CSN derived from commercially available chitosan acquired from Acros Organics (Tarchoun et al. 2022b). This finding suggests the potential effect of chitosan origin, the processing method, and the nitration conditions on the thermal behavior of the resulting energetic chitosan-rich polymer. Besides that, it is clear from Fig. 4a that NC exhibits an abrupt loss of mass (80.1%) at a maximum peak temperature of 204.3 °C, whereas CSN decomposes in two stages. The reduced thermal stability of CSN compared to conventional NC is originated from the presence of both nitrogen-rich and thermally unstable N–NO_2 and O–NO_2 functional groups in CSN, which significantly accelerate its thermal decomposition (Tarchoun et al. 2020b; Chen et al. 2022).

Regarding the newly developed energetic mixtures, it is evident from Fig. 4b that all the elaborated CSN/NC blends generate a large single-step mass loss stage within the temperature range of 179.6–233.9 °C, which is interestingly higher than the thermal decomposition of pure CSN. It can be also revealed that the increase of NC content in CSN/NC mixture leads to an improvement of the thermal stability and mass loss, following the trend of its individual compounds. These findings suggest that the NC thermolysis confers thermal resistance to the CSN decomposition by promoting the heat transfer from the reaction zone to the unburned portions, which delays the propagation of the decomposition process (Tarchoun et al. 2022a; Benhammada et al. 2020). On the other, the early decomposition of CSN/NC mixtures compared to the pure NC is due to the released reactive species and energy during CSN decomposition. These outcomes demonstrate that both CSN and NC may promote the decomposition of each other through a synergistic mechanism, and thus such blend may find effective applications as a binder for solid propellants or as an additive to improve the performance of rocket propellants and composite explosives.

Thermal assessment by DSC

In order to advance the investigation of the thermal behavior of CSN and its precursor (CS), and further evaluate the effect of compounding on the stability and thermal properties of the developed NC/CSN blends for use in practical energetic applications, DSC analyses of the mentioned samples were carried out, and the corresponding thermograms are presented in Fig. 5, while the corresponding data are summarized in Table 1. Similarly to the commercial chitosan purchased from Acros Organics, previously studied in our recent work (Tarchoun et al. 2022b), the thermogram of CS, extracted from shrimp *Parapenaeus longirostris* shells, exhibits a single small exothermic decomposition, with the onset and maximum peak temperatures of 281.4 and 308.1 °C, respectively, reflecting bonds scission within and between glucosamine units of the CS polymer chains (Barbosa et al. 2019; Muñoz–Nuñez et al. 2022).

Table 1 DSC parameters of the analyzed samples at $\beta = 10$ °C/min

Sample	T_{onset} (°C)	T_{peak} (°C)	/ΔH/ (J/g)
CS	275.4	308.1	798
CSN	139.0	T_{peak1} = 159.9 T_{peak2} =212.6	2198
NC	196.4	204.5	1545
CSN 25% NC 75%	187.4	201.7	1784
CSN 50% NC 50%	185.3	205.0	2215
CSN 75% NC 25%	181.2	206.5	2332

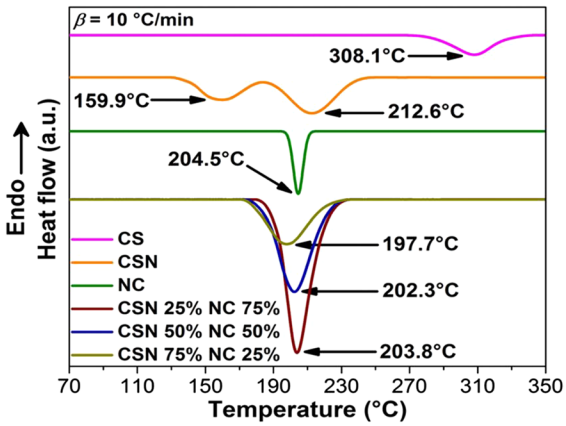

Fig. 5 DSC thermograms of CSN/NC blends and their pure compounds at $\beta = 10$ °C/min

On the other hand, the substitution of free accessible hydroxyl and amino groups by nitrate esters and nitramines, respectively, in CSN causes a decrease in its thermal decomposition accompanied by an interesting increase of its heat release, due to the transition of its starting temperature of decomposition (from T_{onset} = 275.4 °C for CS to T_{onset} = 139.0 °C for CSN) and its enthalpy of reaction (from ΔH = –798 J/g for CS to ΔH = –2198 J/g for CSN). In contrast to CS, CSN presents two consecutive exothermic events within the range of 138–185 °C and 190–235 °C, respectively. the first degradation event, appeared at T_{peak1} = 159.9 °C, is attributed to the thermolytic cleavage of the energetic N–NO_2 and O–NO_2 groups; while the second one, located at T_{peak2} = 212.6 °C, corresponded to the thermo-oxidative destruction of glucosamine units. Moreover, it is evident from Fig. 5; Table 1 that the produced CSN, in addition to its increased nitrogen content, displays a significantly high heat release with basically acceptable thermal decomposition compared to the conventional cellulose nitrate, indicating its superior performance for potential uses in the fields of propulsion and explosives. Therefore, compared to the TGA/DTG results, similar thermal degradation behavior is recorded by DSC.

As for the DSC thermograms of the developed energetic mixtures plotted in Fig. 5, a single exothermic decomposition peak is observed for all CSN/NC blends, which starts at 181–188 °C and proceeds at maximum temperatures ranges of 201–207 °C. We can also denote from Fig. 5; Table 1 that doping CSN by NC leads to an improvement of the thermolysis process toward higher temperatures. Therefore, all the newly developed CSN/NC mixtures show better thermal stability than pure CSN. Moreover, the integration of peak areas shows that the pyrolysis energy (ΔH) released during CSN/NC blends decomposition increases proportionally with the fraction of CSN, highlighting the advantage of adding CSN to overcome the low energy released by NC at its pyrolysis. In fact, CSN/NC blends with a mass ratio in CSN higher than 50% (i.e. CSN 50% NC 50% and CSN 75% NC 25%) reveal higher enthalpy of reaction than pure CSN, which indicates a good synergistic effect between CSN and NC that can be the consequence of the enhanced interfacial contact between CSN and NC matrices, as proved by SEM analysis. This fact also suggests that the burning rate of CSN/NC composites might be improved by the exothermic superficial reactions that occur within the mixture (Mezroua et al. 2022). Additionally, it is important to highlight that the prepared CSN/NC blends have better thermal stability than some reported NC– and CSN-based composites such as NC/GAP (T_{peak} = 193°Cat $\beta = 10$ °C/min) (Luo et al. 2019), NC/HMX (T_{peak} = 168 °C at $\beta = 10$ °C/min) (Wang et al. 2016), CSN/RDX (T_{peak} = 145–150 °C at $\beta = 10$ °C/min) (Li et al. 2020), and CSN/Ti (T_{peak} = 153–155 °C at $\beta = 10$ °C/min) (Zhang et al. 2022). These interesting outcomes established that CSN could be considered an excellent additive for boosting NC to more interesting energetic proprieties, and show that the NC is satisfactory for the improvement of CSN thermal stability.

Physico-chemical properties, combustion parameters, sensitivity characteristics, and energetic performances

In order to further elucidate the characteristics of the designed energetic CSN and CSN/NC blends, their thermodynamic parameters and energetic performance were evaluated and the determined data are summarized in Table 2. Interestingly, CSN, produced in this study from local shrimp shells, presents outstanding density, nitrogen content, energy of combustion, and mechanical insensitivities, which are remarkably better than those of structurally similar nitrocellulose, as well as comparable to those of high-substitute nitrochitosan recently designed by our research group from commercially available chitosan (Tarchoun et al. 2022b). Moreover, the calculated molar enthalpies of formation ($\Delta_f H$) show that the investigated energetic CSN and NC binders have negative $\Delta_f H$, highlighting the exothermic reaction of formation of these energetic polysaccharides from the basic elements. Another interesting finding is that the synthesized CSN has a much higher density than the common energetic polymers such as glycidyl azide polymer (GAP: 1.30 g/cm^3) (Wu et al. 2020), poly(glycidyl nitrate) (Poly GLYN: 1.46 g/cm^3) (Yan et al. 2016), and some emergent energetic poly(ionic liquids) (1.60–1.65 g/cm^3) (Wang et al. 2018). In addition, EXPLO5 (V6.04) thermodynamic program was utilized to compute the detonation parameters, according to the Chapman–Jouguet (CJ) theory, and the specific impulse (I_{sp}), calculated under isobaric conditions at 7 MPa, of the studied energetic polysaccharide. Interestingly, the computational data, reported in Table 2, reveal that the designed CSN from shrimp shells has better heat of detonation ($\Delta_E U^0$), detonation velocity (D_{C-J}), temperature of explosion (T_{C-J}), and I_{sp} than the commonly employed NC, and GAP ($\Delta_E U^0$= 4307 kJ/kg, D_{C-J} = 6638 m/s, T_{C-J} = 2404 K, I_{sp} = 207 s) (Betzler et al. 2016), which are even superior to those of new energetic nitrogen-rich cellulosic polymers including 6-deoxy-6-(ω-aminoethyl)nitramino cellulose nitrate ($\Delta_E U^0$= 4774 kJ/kg, D_{C-J} = 7576 m/s, T_{C-J} = 2867 K, I_{sp} = 211 s) (Tarchoun et al. 2020b), azidodeoxy-cellulose nitrate ($\Delta_E U^0$= 4715 kJ/kg, D_{C-J} = 7533 m/s, T_{C-J} = 3038 K, I_{sp} = 215 s) (Tarchoun et al. 2020c), and 2-(1 H-tetrazol-1-yl)acetate cellulose nitrate ($\Delta_E U^0$= 4680 kJ/kg, D_{C-J} = 7552 m/s, T_{C-J} = 3033 K, I_{sp} = 212 s) (Tarchoun et al. 2021a). These outcomes highlight the potential valorization of *Parapenaeus longirostris* shrimp wastes as valuable marine co-products to develop a promising energetic nitrogen-rich polysaccharide (CSN) for futuristic high-performance energetic formulations.

In the case of the newly developed energetic mixtures, an interesting finding that one can reveal from Table 2 is that CSN/NC blends display greater density and energy of combustion than those of pure energetic polymers. The increase of these parameters will certainly enhance the overall performance of the

Table 2 Energetic performance of the developed CSN and its blend with NC.

	CSN	NC	CSN 25% NC 75%	CSN 50% NC 50%	CSN 75% NC 25%
ρ [a] (g/cm^3)	1.701 ± 0.003	1.671 ± 0.004	1.735 ± 0.002	1.849 ± 0.003	1.835 ± 0.002
Nc [b] (%, w/w)	16.55 ± 0.05	12.61 ± 0.04	–	–	–
IS [c] (J)	15	3	10	15	15
FS [d] (N)	> 360	350	> 360	> 360	> 360
$\Delta_c U$ [e] (J/g)	–10,605	–9205	–10,816	–11,953	–11,609
$\Delta_f H$ [f] (kJ/mol)	–468	–710	–649	–588	–528
$\Delta_E U^0$ [g] (kJ/kg)	–5070	–4743	–4885	–4987	–5023
D_{C-J} [h] (m/s)	7769	7446	7620	7715	7735
P_{C-J} [i] (GPa)	25	24	24	25	25
T_{C-J} [j] (K)	3450	3405	3420	3438	3443
I_{sp} [k] (s)	244	235	240	242	243

[a] Density derived from electronic densimeter, [b] Nitrogen content derived from elemental analysis, [c] BAM impact tester, [d] BAM friction tester, [e] Experimental combustion energy (constant volume), [f] Calculated molar enthalpy of formation, [g] Heat of detonation, [h] Detonation velocity, [i] Detonation pressure, [j] Temperature of detonation, [k] Specific impulse (isobaric combustion, chamber pressure 70 bar, frozen expansion)

energetic formulation. Furthermore, all the designed CSN/NC blends are found to be friction insensitive; whereas, they show relative impact insensitivity similar to that of CSN but interestingly better than that of NC, benefiting from the synergistic effect and the excellent interfacial contact between CSN and NC. The uniform dispersion of both CSN and NC would also reduce the formation of hot spots, and thus improve the insensitivity of the blend. Another important finding is that all the elaborated CSN/NC blends produce satisfactory $\Delta_E U^0$, D_{C-J}, T_{C-J}, and I_{sp} parameters, which are boosted with increasing CSN content, showing that the introduction of CSN, even at a low mass fraction (25 wt%), improves the energetic performance of NC. The enhancement of the energetic features means that an effective and highly energetic composite can be designed based on CSN/NC binder. In addition, all the reported CSN/NC blends present better D_{C-J} than some explosives including Trinitrotoluene (TNT: D_{C-J} = 6900 m/s) (Muravyev et al. 2022), and Hexanitrostilbene (HNS: D_{C-J} = 7612 m/s) (Tang et al. 2020), as well as higher I_{sp} than some currently employed solid rocket propellants ($I_{sp} \approx$ 220–225 s) (Elbasuney et al. 2017; Chalghoum et al. 2022). We can also deduce from Table 2 that, compared to the CSN/NC blend with a mass ratio (wt%) of 50:50. The introduction of 75 wt% CSN does not significantly affect the energetic parameters, which suggests that the optimal fraction is around the equi-mass ((wt%) = 50:50). Based on the above results, we can conclude that both CSN and NC may positively affect the physical stability and the energetic performance of each other *via* a synergistic effect, and thus such blend can find effective application in the area of solid rocket propellants and explosive.

Conclusions

During this study, we demonstrated that the residues from shrimp *Parapenaeus longirostris* shells can be effectively valorized to develop a promising energetic nitrogen-rich polysaccharide through electrophilic nitration of the extracted chitosan. The high purity and the successful molecular structure of the designed energetic CSN and its extracted CS and CT precursors were confirmed by elemental analysis and structural measurements. Importantly, the designed CSN from local shrimp shells displayed remarkedly improved density, nitrogen content, heat of combustion, mechanical insensitivities, and energetic performance, as well as fundamentally acceptable thermal decomposition compared to the commonly used NC. Additionally, new energetic blends based on CSN and NC, with different mass ratios (CSN:NC (wt.%) = 25:75, 50:50, and 25:75), were elaborated and fully characterized. FTIR and SEM results demonstrated the homogeneity of the developed CSN/NC blends without obvious defects. Compared to pure CSN and NC, all the prepared CSN/NC blends exhibited increased density, heat of combustion, and enthalpy of reaction. Furthermore, the decomposition temperatures of CSN/NC blends are found to be interestingly higher than that of pure CSN, highlighting the positive effect of the introduction of NC. It was also revealed that all CSN/NC mixtures possess satisfactory impact and friction sensitivities, similar to that of CSN, but attractively better than that of NC. Additionally, the computed theoretical energetic performance showed that the new elaborated energetic blends provide great detonation velocity (7674 m/s $\leq D_{C-J} \leq$ 7761 m/s) and specific impulse (241 s $\leq I_{sp} \leq$ 248 s), demonstrating that both CSN and NC could effectively enhance the energetic properties of each other through a synergistic mechanism. Above all, we participated through the present study in paving the way toward promising energetic polysaccharide derived from local marine *Parapenaeus longirostris* wastes, which has not been addressed yet, and we also provided new insights into advantageous characteristics of CSN/NC blends for future applications in advanced high-performance energetic formulations. As such, the interactions of CSN and its chemical compatibility with other additives to develop the next generation of energetic composites should remain among the main foci of the postulated next stage of research on those promising materials.

Acknowledgments Financial support of this research by the Ecole Militaire Polytechnique is gratefully acknowledged.

Author contribution A.F.T.: Conceptualization, Methodology, Resources, Investigation, data treatment, Writing-Original Draft. D.T.: Conceptualization, Review & Editing. A.H., A.A.,

H.B., I.C., S.T. and T.M.K.: Review & Editing the manuscript draft. All authors have approved the final version of the article.

Funding The authors declare that they have received no specific grant from any funding agency in the public, commercial, or not-for-profit sectors.

Data availability All data supporting the findings of this study are available within the article.

Declaration

Conflicts of interest The authors declare that they have no conflicts of interest with respect to the research, authorship, and/or publication of this article.

Ethical approval All authors state that they adhere to the Ethical Responsibilities of Authors.

Informed consent Informed consent was obtained from all individual participants included in the study.

Research involving human participants and/or animals This article does not contain any studies with human participants or animals performed by any of the authors.

References

Ahmad A, Mubarak N, Naseem K, Tabassum H, Rizwan M, Najda A, Kashif M, Bin-Jumah M, Hussain A, Shaheen A (2020) Recent advancement and development of chitin and chitosan-based nanocomposite for drug delivery: critical approach to clinical research. Arab J Chem 13(12):8935–8964

Barbosa HF, Francisco DS, Ferreira AP, Cavalheiro ÉT (2019) A new look towards the thermal decomposition of chitins and chitosans with different degrees of deacetylation by coupled TG-FTIR. Carbohydr Polym 225:115232

Begum S, Yuhana NY, Saleh NM, Kamarudin NHN, Sulong AB (2021) Review of chitosan composite as a heavy metal adsorbent: material preparation and properties. Carbohydr Polym 259:117613

Ben Seghir B, Benhamza M (2017) Preparation, optimization and characterization of chitosan polymer from shrimp shells. J Food Meas Charact 11(3):1137–1147

Benhabiles M, Salah R, Lounici H, Drouiche N, Goosen M, Mameri N (2012) Antibacterial activity of chitin, chitosan and its oligomers prepared from shrimp shell waste. Food Hydrocoll 29(1):48–56

Benhammada A, Trache D, Kesraoui M, Chelouche S (2020) Hydrothermal synthesis of hematite nanoparticles decorated on carbon mesospheres and their synergetic action on the thermal decomposition of nitrocellulose. Nanomaterials 10(5):968

Betzler FM, Hartdegen VA, Klapötke TM, Sproll SM (2016) A new energetic binder: glycidyl nitramine polymer. Cent Eur J Energ Mater 13(2):289–300

Bhardwaj S, Bhardwaj NK, Negi YS (2021) Surface coating of chitosan of different degree of acetylation on non surface sized writing and printing grade paper. Carbohydr Polym 269:117674

Chalghoum F, Trache D, Benziane M, Chelouche S (2022) Effect of complex metal hydride on the thermal decomposition behavior of AP/HTPB-based aluminized solid rocket propellant. J Therm Anal Calorim 147(20):11507–11534

Chen F, Wang Y, Zhang Q (2022) Recent advances in the synthesis and properties of energetic plasticizers. New J Chem 46(43):20540–20553

da Silva Lucas AJ, Oreste EQ, Costa HLG, Lopez HM, Saad CDM, Prentice C (2021) Extraction, physicochemical characterization, and morphological properties of chitin and chitosan from cuticles of edible insects. Food Chem 343:128550

Doğdu SA, Turan C, Depci T (2021) Extraction and characterization of chitin and Chitosan from invasive alien swimming crab Charybdis longicollis. Nat Eng Sci 6(2):96–101

Domszy JG, Roberts GA (1985) Evaluation of infrared spectroscopic techniques for analysing chitosan. Die Makromol Chem Macromol Chem Phys 186(8):1671–1677

Dou J, Xu M, Tan B, Lu X, Mo H, Wang B, Liu N (2022) Research progress of nitrate ester binders. Fire Phys Chem 3(1):54–77

El Knidri H, Belaabed R, Addaou A, Laajeb A, Lahsini A (2018) Extraction, chemical modification and characterization of chitin and chitosan. Int J Biol Macromol 120:1181–1189

Elbasuney S, Fahd A, Mostafa HE (2017) Combustion characteristics of extruded double base propellant based on ammonium perchlorate/aluminum binary mixture. Fuel 208:296–304

Flórez M, Guerra-Rodríguez E, Cazón P, Vázquez M (2022) Chitosan for food packaging: recent advances in active and intelligent films. Food Hydrocoll 124:107328

Francis AO, Zaini MAA, Muhammad IM, Abdulsalam S, El-Nafaty UAJBC, Biorefinery (2021) Physicochemical modification of chitosan adsorbent: a perspective. Biomass Convers Biorefin. https://doi.org/10.1007/s13399-021-01599-3

Guo M, Ma Z, He L, He W, Wang Y (2017) Effect of varied proportion of GAP-ETPE/NC as binder on thermal decomposition behaviors, stability and mechanical properties of nitramine propellants. J Therm Anal Calorim 130(2):909–918

Huet G, Hadad C, González-Domínguez JM, Courty M, Jamali A, Cailleu D, van Nhien AN (2021) IL versus DES: impact on chitin pretreatment to afford high quality and highly functionalizable chitosan. Carbohydr Polym 269:118332

Jha PK, Halada GP, McLennan SM (2013) Electrochemical synthesis of nitro-chitosan and its performance in chromium removal. Coatings 3(3):140–152

Joseph SM, Krishnamoorthy S, Paranthaman R, Moses J, Anandharamakrishnan C (2021) A review on source-specific chemistry, functionality, and applications of chitin and chitosan. Carbohydr Polym Technol Appl 2:100036

Kasaai MR (2008) A review of several reported procedures to determine the degree of N-acetylation for chitin and

chitosan using infrared spectroscopy. Carbohydr Polym 71(4):497–508
Kaya M, Baran T, Mentes A, Asaroglu M, Sezen G, Tozak KO (2014) Extraction and characterization of α-chitin and chitosan from six different aquatic invertebrates. Food Biophys 9(2):145–157
Kumari S, Annamareddy SHK, Abanti S, Rath PK (2017) Physicochemical properties and characterization of chitosan synthesized from fish scales, crab and shrimp shells. Int J Biol Macromol 104:1697–1705
Lavall RL, Assis OB, Campana-Filho SP (2007) β-Chitin from the pens of Loligo sp.: extraction and characterization. Bioresour Technol 98(13):2465–2472
Li C, Li H, Xu K (2020) High-substitute Nitrochitosan used as energetic materials: Preparation and Detonation Properties. Carbohydr Polym 237:116176
Liakos EV, Lazaridou M, Michailidou G, Koumentakou I, Lambropoulou DA, Bikiaris DN, Kyzas GZ (2021) Chitosan adsorbent derivatives for pharmaceuticals removal from effluents: a review. Macromol 1(2):130–154
Liu H, Zhang L (2001) Structure and properties of semiinterpenetrating polymer networks based on polyurethane and nitrochitosan. J Appl Polym Sci 82(12):3109–3117
Luo T, Wang Y, Huang H, Shang F, Song X (2019) An electrospun preparation of the NC/GAP/nano-LLM-105 nanofiber and its properties. Nanomaterials 9(6):854
Luo Q, Hong J, Xu H, Han S, Tan H, Wang Q, Tao J, Ma N, Cheng Y, Su H (2020) Hygroscopicity of amino acids and their effect on the water uptake of ammonium sulfate in the mixed aerosol particles. Sci Total Environ 734:139318
Marei NH, Abd El-Samie E, Salah T, Saad GR, Elwahy AHJIjobm (2016) Isolation and characterization of chitosan from different local insects in Egypt. Int J Biol Macromol 82:871–877
Mezroua A, Hamada RA, Brahmine KS, Abdelaziz A, Tarchoun AF, Boukeciat H, Bekhouche S, Bessa W, Benhammada A, Trache D (2022) Unraveling the role of ammonium perchlorate on the thermal decomposition behavior and kinetics of NC/DEGDN energetic composite. Thermochim Acta 716:179305
Mohan K, Ganesan AR, Muralisankar T, Jayakumar R, Sathishkumar P, Uthayakumar V, Chandirasekar R, Revathi N (2020) Recent insights into the extraction, characterization, and bioactivities of chitin and chitosan from insects. Trends Food Sci Technol 105:17–42
Mohanty AK, Wu F, Mincheva R, Hakkarainen M, Raquez J-M, Mielewski DF, Narayan R, Netravali AN, Misra M (2022) Sustainable polymers. Nat Rev Methods Prim 2(1):1–27
Muñoz-Nuñez C, Cuervo-Rodríguez R, Echeverría C, Fernández-García M, Muñoz-Bonilla A (2022) Synthesis and characterization of thiazolium chitosan derivative with enhanced antimicrobial properties and its use as component of chitosan based films. Carbohydr Polym 302:120438
Muravyev NV, Wozniak DR, Piercey DG (2022) Progress and performance of energetic materials: open dataset, tool, and implications for synthesis. J Mater Chem A 10(20):11054–11073
Nasrollahzadeh M, Sajjadi M, Iravani S, Varma RS (2021) Starch, cellulose, pectin, gum, alginate, chitin and chitosan derived (nano) materials for sustainable water treatment: a review. Carbohydr Polym 251:116986
Negm NA, Hefni HH, Abd-Elaal AA, Badr EA, Abou Kana MT (2020) Advancement on modification of chitosan biopolymer and its potential applications. Int J Biol Macromol 152:681–702
Olaosebikan AO, Kehinde OA, Tolulase OA, Victor EB (2021) Extraction and characterization of chitin and chitosan from callinectes amnicola and penaeus notialis shell wastes. J Chem Eng Mater Sci 12(12):1–30
Pal K, Bharti D, Sarkar P, Anis A, Kim D, Chałas R, Maksymiuk P, Stachurski P, Jarzębski M (2021) Selected applications of chitosan composites. Int J Mol Sci 22(20):10968
Phuong PTD, Trung TS, Stevens WF, Minh NC, Bao HND, Hoa NV (2022) Valorization of heavy waste of modern intensive shrimp farming as a potential source for chitin and chitosan production. Waste Biomass Valoriz 13(2):823–830
Rahman NA, Abu Hanifah S, Mobarak NN, Su'ait MS, Ahmad A, Shyuan LK, Khoon LT (2019) Synthesis and characterizations of o-nitrochitosan based biopolymer electrolyte for electrochemical devices. PLoS ONE 14(2):e0212066
Rashki S, Asgarpour K, Tarrahimofrad H, Hashemipour M, Ebrahimi MS, Fathizadeh H, Khorshidi A, Khan H, Marzhoseyni Z, Salavati-Niasari M (2021) Chitosan-based nanoparticles against bacterial infections. Carbohydr Polym 251:117108
Rasweefali M, Sabu S, Sunooj K, Sasidharan A, Xavier KM (2021) Consequences of chemical deacetylation on physicochemical, structural and functional characteristics of chitosan extracted from deep-sea mud shrimp. Carbohydr Polym Technol Appl 2:100032
Reshmy R, Philip E, Madhavan A, Sirohi R, Pugazhendhi A, Binod P, Awasthi MK, Vivek N, Kumar V, Sindhu R (2022) Lignocellulose in future biorefineries: strategies for cost-effective production of biomaterials and bioenergy. Bioresour Technol 344:126241
Saravana PS, Ho TC, Chae S-J, Cho Y-J, Park J-S, Lee H-J, Chun B-S (2018) Deep eutectic solvent-based extraction and fabrication of chitin films from crustacean waste. Carbohydr Polym 195:622–630
Srinivasan H, Kanayairam V, Ravichandran RJIjobm (2018) Chitin and chitosan preparation from shrimp shells Penaeus monodon and its human ovarian cancer cell line, PA-1. Int J Biol Macromol 107:662–667
Tang Y, Yin Z, Chinnam AK, Staples RJ, Shreeve JnM (2020) A duo and a trio of triazoles as very thermostable and insensitive energetic materials. Inorg Chem 59(23):17766–17774
Tarchoun AF, Trache D, Klapötke TM (2019a) Microcrystalline cellulose from Posidonia oceanica brown algae: extraction and characterization. Int J Biol Macromol 138:837–845
Tarchoun AF, Trache D, Klapötke TM, Derradji M, Bessa W (2019b) Ecofriendly isolation and characterization of microcrystalline cellulose from giant reed using various acidic media. Cellulose 26(13–14):7635–7651
Tarchoun AF, Trache D, Klapötke TM, Belmerabet M, Abdelaziz A, Derradji M, Belgacemi R (2020a) Synthesis, characterization, and thermal decomposition kinetics of nitrogen-rich energetic biopolymers from

aminated giant reed cellulosic fibers. Ind Eng Chem Res 59(52):22677–22689
Tarchoun AF, Trache D, Klapötke TM, Krumm B (2020b) New insensitive nitrogen-rich energetic polymers based on amino-functionalized cellulose and microcrystalline cellulose: synthesis and characterization. Fuel 277:118258
Tarchoun AF, Trache D, Klapötke TM, Krumm B, Khimeche K, Mezroua A (2020c) A promising energetic biopolymer based on azide-functionalized microcrystalline cellulose: synthesis and characterization. Carbohydr Polym 249:116820
Tarchoun AF, Trache D, Klapötke TM, Abdelaziz A, Derradji M, Bekhouche S (2021a) Chemical design and characterization of cellulosic derivatives containing high-nitrogen functional groups: towards the next generation of energetic biopolymers. Def Technol 18(4):537–546
Tarchoun AF, Trache D, Klapötke TM, Selmani A, Saada M, Chelouche S, Mezroua A, Abdelaziz A (2021b) New insensitive high-energy dense biopolymers from giant reed cellulosic fibers: their synthesis, characterization, and non-isothermal decomposition kinetics. New J Chem 45(11):5099–5113
Tarchoun AF, Trache D, Abdelaziz A, Harrat A, Boukecha WO, Hamouche MA, Boukeciat H, Dourari M (2022a) Elaboration, characterization and thermal decomposition kinetics of new nanoenergetic composite based on hydrazine 3-Nitro-1, 2, 4-triazol-5-one and nanostructured cellulose nitrate. Molecules 27(20):6945
Tarchoun AF, Trache D, Hamouche MA, Bessa W, Abdelaziz A, Boukeciat H, Bekhouche S, Belmehdi D (2022b) Insights into characteristics and thermokinetic behavior of potential energy-rich polysaccharide based on chitosan. Cellulose 29(15):8085–8101
Tarchoun AF, Trache D, Klapötke TM, Abdelaziz A, Bekhouche S, Boukeciat H, Sahnoun N (2022c) Making progress towards promising energetic cellulosic microcrystals developed from alternative lignocellulosic biomasses. J Energ Mater. https://doi.org/10.1080/07370652.2022.2032484
Tarchoun AF, Trache D, Klapötke TM, Slimani K, Belouettar Be, Abdelaziz A, Bekhouche S, Bessa W (2022d) Valorization of esparto grass cellulosic derivatives for the development of promising energetic azidodeoxy biopolymers: synthesis, characterization and isoconversional thermal kinetic analysis. Propellants Explos Pyrotech 47(3):e202100293
Teli M, Sheikh JJIjobm (2012) Extraction of chitosan from shrimp shells waste and application in antibacterial finishing of bamboo rayon. Int J Biol Macromol 50:1195–12005
Touidjine S, Boulkadid KM, Trache D, Belkhiri S, Mezroua A (2022) Preparation and characterization of polyurethane/nitrocellulose blends as binder for composite solid propellants. Propellants Explos Pyrotech 47(1):e202000340
Trache D, Tarchoun AF (2019) Differentiation of stabilized nitrocellulose during artificial aging: spectroscopy methods coupled with principal component analysis. J Chemom 33(8):e3163
Trung TS, Van Tan N, Van Hoa N, Minh NC, Loc PT, Stevens WF (2020) Improved method for production of chitin and chitosan from shrimp shells. Carbohydr Res 489:107913
Wang Y, Song X, Song D, Liang L, An C, Wang J (2016) Synthesis, thermolysis, and sensitivities of HMX/NC energetic nanocomposites. J Hazard Mater 312:73–83
Wang B, Feng Y, Qi X, Deng M, Tian J, Zhang Q (2018) Designing explosive poly (ionic liquid) s as novel energetic polymers. Chem A Eur J 24(59):15897–15902
Wu Q, Ma Q, Zhang Z, Yang W, Gou S, Huang J, Fan G (2020) Combustion and catalytic performance of metal-free heat-resistant energetic polymeric materials. Chem Eng J 399:125739
Yan Q-L, Cohen A, Chinnam AK, Petrutik N, Shlomovich A, Burstein L, Gozin M (2016) A layered 2D triaminoguanidine–glyoxal polymer and its transition metal complexes as novel insensitive energetic nanomaterials. J Mater Chem A 4(47):18401–18408
Yuan Y, Hong S, Lian H, Zhang K, Liimatainen H (2020) Comparison of acidic deep eutectic solvents in production of chitin nanocrystals. Carbohydr Polym 236:116095
Zhang L, Chen P, Huang J, Yang G, Zheng L (2003) Ways of strengthening biodegradable soy-dreg plastics. J Appl Polym Sci 88(2):422–427
Zhang W, Qin Z, Yi J, Chen S, Xu K (2022) Laser ignition and combustion properties of composite with high-substituted nitrochitosan and nano-Ti powder. Combust Flame 240:112056
Zhao D, Huang W-C, Guo N, Zhang S, Xue C, Mao X (2019) Two-step separation of chitin from shrimp shells using citric acid and deep eutectic solvents with the assistance of microwave. Polymers 11(3):409
Aili D, Arbia W, Adour L (2017) Treatment of colored waters by beads chitosan, extracted from shrimp waste. In: International symposium on materials and sustainable development. Springer, Cham, p 492–505
NATO SA (1999) 4489 (STANAG 4489), explosives. Impact Sensitivity Tests
NATO SA (2002) 4487 (STANAG 4487), explosives. Friction Sensitivity Tests
Sućeska M (2017) EXPLO5 V6. Brodarski Institute: Zagreb, p 04